2014 IEEE International Conference on Robotics & Automation (ICRA)
Hong Kong Convention and Exhibition Center
May 31 - June 7, 2014. Hong Kong, China

Variable Stiffness Treadmill (VST): a Novel Tool for the Investigation of Gait

Andrew Barkan, Jeffrey Skidmore and Panagiotis Artemiadis*

Abstract— **Locomotion is one of the human's most important functions that serve survival, progress and interaction. Gait requires kinematic and dynamic coordination of the limbs and muscles, multi-sensory fusion and robust control mechanisms. The force stimulus generated by the interaction of the foot with the walking surface is a vital part of the human gait. Although there have been many studies trying to decipher the load feedback mechanisms of gait, there is a need for the development of a versatile system that can advance research and provide new functionality. In this paper, we present the design and characterization of a novel system, called Variable Stiffness Treadmill (VST). The device is capable of controlling load feedback stimulus by regulating the walking surface stiffness in real time. The high range of available stiffness, the resolution and accuracy of the device, as well as the ability to regulate stiffness within the stance phase of walking, are some of the unique characteristics of the VST. We present experiments with healthy subjects in order to prove the concept of our device and preliminary findings on the effect of altered stiffness on gait kinematics. The developed system constitutes a uniquely useful research tool, which can improve our understanding of gait and create new avenues of research on gait analysis and rehabilitation.**

I. Introduction

Stimulus is a vital part of the human gait mechanisms. It is the feedback that governs the way we operate in our complex and evolving environment. In human gait motion, there are many forms of stimulus; however, each type of stimulus holds essential information, without which, proper gait motion would be an impossible task. While the effect of load feedback (an important stimulus) on gait has been an active field of study (for example [1]–[9]), there is a need for the development of a versatile system that can advance research in this area by providing new functionality.

In previous studies, researchers have utilized compliant surfaces to investigate the effect of load feedback on gait. The simplest setups include surfaces created out of foam of varying stiffness [10], [11], or collegiate gym mats [12]. However, inherent in these setups is the inability to utilize a large range of stiffness while maintaining high resolution (without employing an extreme number of materials).

The development of devices that allow for easy adjustment of stiffness between experiments began decades ago by McMahon and Greene [13]. Their setup included simply supported plywood boards where the stiffness is changed by adjusting the distance between the two supports [13]. More recently, Kerdok et al. also utilized the concept of the deformation of a supported compliant beam in their development of a compliant track treadmill [14]. While improving the easiness and resolution of compliant walking surfaces, these designs do not allow for the compliance of the surface to be changed in situ. Moreover, there is no ability to exert a prescribed force perturbation to the foot in real time while a subject is actively walking on the surface.

In order to address the gaps left by other devices, a novel system, called Variable Stiffness Treadmill (VST), has been developed with several advantages over existing devices. First of all, the VST has a wide range of controllable stiffness (essentially zero to infinite), but maintains high resolution. Second, it has the ability to actively vary and control the compliance of the treadmill surface within the gait cycle. Unlike previous devices, the VST is capable of creating any profile of stiffness during an experiment and throughout the gait cycle. Third, by measuring the displacement of the walking surface, we can not only estimate the load force exerted on the foot, but can also exert a force on the foot by adjusting the stiffness in real-time. The above elements allow for a better understanding of gait. The novel setup we developed allows for a large range of selectable stiffness throughout the gait cycle, as well as for full-continuous control of that stiffness during the stance phase. This allows the introduction of a plethora of force perturbations to the leg that are impossible to implement with current devices.

In this paper, we introduce the VST system by presenting its design characteristics, its governing equations, and results of initial experiments. We first present the concept of variable stiffness and the mechanism used to control it. We analyze its governing equations of motion and functionality. Then, we analyze all the subsystems of the total device that allow the real-time operation. Experiments with human subjects were designed in order to prove the concept of our device. We present experimental data that shows the efficiency of the system and preliminary data on the effect of altered stiffness on gait kinematics. The proposed system constitutes the first mechanical device that can alter the walking surface stiffness in real-time, with accuracy, resolution and robustness. The latter characteristics provide a uniquely useful research tool, which can improve our understanding of gait and create new avenues of research on gait analysis and rehabilitation.

The rest of the paper is organized as follows: Section II details the structure and governing equations of the device, as well as its technical specifications. Section III presents proof-of-concept experiments using the VST on healthy subjects. Finally, section IV concludes the paper with a brief discussion and summary of the contribution.

*Corresponding author
All authors are with the Department of Mechanical and Aerospace Engineering, Arizona State University, Tempe, AZ 85287, USA {abarkan, jaskidmo, panagiotis.artemiadis}@asu.edu

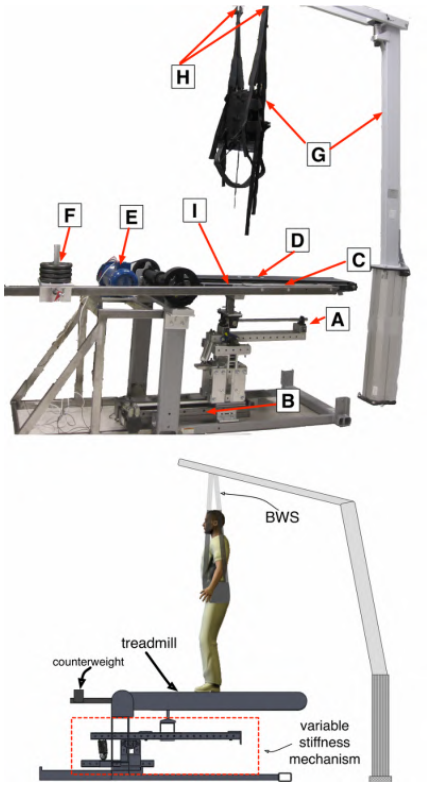

Fig. 1. The VST setup. Actual platform (top) and conceptual diagram (bottom). Subsystems shown include: A) Variable stiffness mechanism, B) Linear Track, C) Force sensor mat, D) Split treadmill, E) Treadmill motor, F) Counter-weight system, G) Custom-made harness-based body-weight support, H) Loadcells, I) Inclinometer for treadmill inclination measurement.

II. Methods

A. Design Characteristics

The VST achieves greater versatility and functionality than other devices by combining a variety of components into one unique system. The device is shown in Fig 1. The major components of the VST include a variable stiffness mechanism, a linear track (Thomson Linear Inc), a force sensor mat, a split belt treadmill, a DC treadmill motor (Anaheim Automation), a counter-weight system, and a custom-built body weight support (LiteGait) with two loadcells measuring the subject's weight supported by the system. Each component is important to the system for the overall function and proper investigation of gait, and will be analyzed below.

B. Variable Stiffness Mechanism

The main novel feature of the VST is the ability to vary the vertical stiffness of the walking surface (i.e. treadmill), therefore controlling the force interaction between the walker and the walking surface. The capability of the VST to achieve a large range of controllable stiffness with high resolution comes from a novel variable stiffness mechanism. In its most simplified form, the variable stiffness mechanism is a spring-loaded lever mounted on a translational track, as shown in Fig. 2. The effective stiffness of the treadmill, located at a distance x from the pivot joint, is dependent on the

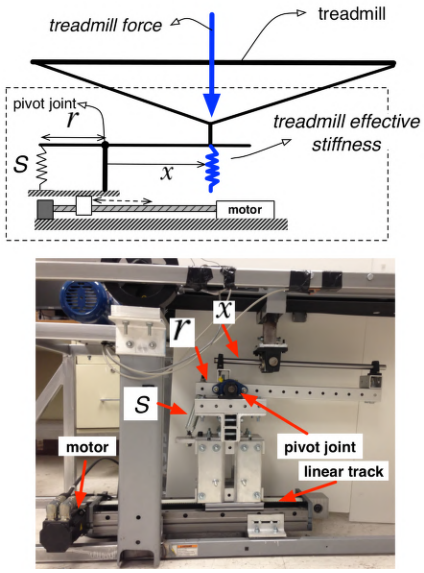

Fig. 2. The variable stiffness mechanism. Conceptual diagram (top) and actual setup (bottom).

coefficient of stiffness S of the linear spring and the moment arm r through which it exerts a force [15]. By design, S and r remain constant, therefore, the effective stiffness of the treadmill can be controlled by changing the distance x.

In order to get our desired range of stiffness, we built the variable stiffness mechanism (Fig. 2) with two extension springs of stiffness $k = 5122N/m$, rest length of $12.7cm$ and outside diameter of $2.54cm$ (LE 135J 06 M, Lee Spring Co.). The two springs are combined in parallel, at a distance of $7.5cm$ from the pivot point. The spring stiffness was chosen to meet our specification for the range of effective treadmill stiffness, which is analyzed below.

This entire assembly sits on the carriage of a high-capacity linear track (Thomson Linear, Part Number: 2RE16-150537) which is controlled by a high-precision drive (Kollmorgen, Part Number: AKD-P00606-NAEC-0000) and has a translational resolution of $0.01mm$. This results in a high resolution for the adjustment of effective stiffness that is discussed below.

In addition to achieving the desired range and resolution of stiffness with the variable stiffness mechanism, we can also vary the treadmill stiffness actively throughout the gait cycle. In the most extreme scenario of going from a rigid surface, i.e. treadmill stiffness of $K_t = \infty$, to the minimum achievable stiffness, the linear track will have to move across its entire range (0 to $40cm$). Considering the fact that the linear track can move as fast as $3m/s$, the system could make this extreme change in stiffness in $0.13s$. Assuming that the subject is walking at a normal pace of $1.4m/s$ [16], [17], with a stride length (the distance between consecutive points of initial contact by the same foot) of $1.4m$ [18], the stance phase would last approx. $0.5s$. This means that the variable stiffness mechanism can make this extreme change in stiffness three times during the stance phase. Therefore, it can easily change stiffness many times throughout the gait

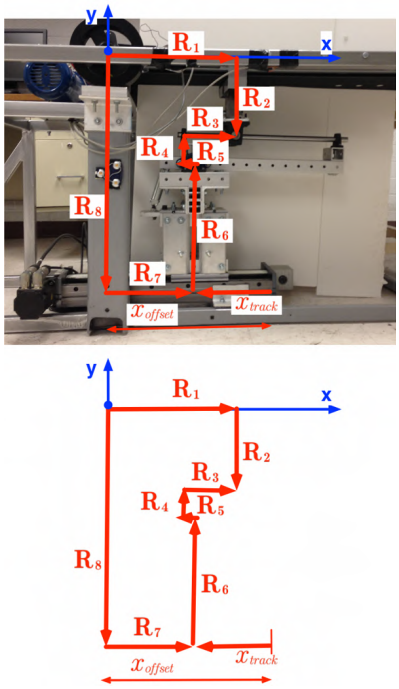

Fig. 3. Kinematic analysis of variable stiffness mechanism.

cycle when the desired change in stiffness is smaller than the two extremes. The ability to change stiffness at a high rate throughout the stance phase of the gait cycle adds to the unique capabilities of the VST.

C. Governing Equations

1) Kinematics: A kinematic analysis of the VST was performed in order to create a mathematical model relating the measured inputs: angular deflection of the treadmill (θ_1), linear track position (x_{track}), and foot position (x_f), to the effective treadmill stiffness at the location of the foot. To accomplish this, the vector loop shown in Fig. 3 was created based off of the rigid body structure of the VST. The vector loop equations are given by:

$$\mathbf{R_1}+\mathbf{R_2}=\mathbf{R_8}+\mathbf{R_7}+\mathbf{R_6}+\mathbf{R_5}+\mathbf{R_4}+\mathbf{R_3} \tag{1}$$

where $\mathbf{R_i}$, $i = 1, 2, \ldots, 8$ are the vectors shown in Fig. 3. Resolving this vector equation into its x and y components using the reference system shown in Fig. 3, we have:

$$\begin{aligned} \sum_{i=1,2} \|\mathbf{R}_i\| \cos(\theta_i) &= \sum_{m=3,4,5,6,7,8} \|\mathbf{R}_m\| \cos(\theta_m) \\ \sum_{i=1,2} \|\mathbf{R}_i\| \sin(\theta_i) &= \sum_{m=3,4,5,6,7,8} \|\mathbf{R}_m\| \sin(\theta_m) \end{aligned} \tag{2}$$

where θ_i, $i = 1, 2, \ldots, 8$ are the angles of the vectors $\mathbf{R_i}$, $i = 1, 2, \ldots, 8$ from the positive x-axis, measured counterclockwise. Some of the vectors are not rotating due to structural constraints listed in Table I. Because of this, the kinematic equations in (2) are simplified to:

TABLE I

KINEMATIC CONTRAINTS

Vector magnitudes (m)		Vector angles (rad)	
$\|\mathbf{R_1}\|$	0.33	θ_6	$\frac{\pi}{2}$
$\|\mathbf{R_2}\|$	0.18	θ_7	0
$\|\mathbf{R_4}\|$	0.085	θ_8	$\frac{-\pi}{2}$
$\|\mathbf{R_5}\|$	0.02	θ_{3a}	0
$\|\mathbf{R_6}\|$	0.44	θ_{4a}	$\frac{\pi}{2}$
$\|\mathbf{R_8}\|$	0.705	θ_2	$\theta_1-\frac{\pi}{2}$
$\|\mathbf{R_{2a}}\|$	0.075	θ_5	$\theta_3-\pi$
$\|\mathbf{R_{3a}}\|$	0.11	θ_4	$\theta_3+\frac{\pi}{2}$
x_{offset}	0.325		
$\|\mathbf{R_{4a}}\|$	0.12	θ_{2a}	θ_3
$\|\mathbf{R_7}\|$	$x_{offset}-x_{track}$		

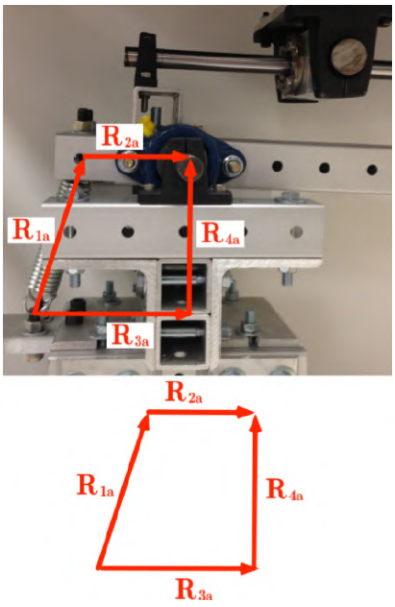

Fig. 4. Kinematic analysis of spring mechanism.

$$\begin{aligned} &\|\mathbf{R_1}\| c_1 + \|\mathbf{R_2}\| s_1 = \\ &\quad x_{offset} - x_{track} - \|\mathbf{R_5}\| c_3 - \|\mathbf{R_4}\| s_3 + \|\mathbf{R_3}\| c_3 \\ &\|\mathbf{R_1}\| s_1 - \|\mathbf{R_2}\| c_1 = \\ &\quad -\|\mathbf{R_8}\| + \|\mathbf{R_6}\| - \|\mathbf{R_5}\| s_3 + \|\mathbf{R_4}\| c_3 + \|\mathbf{R_3}\| s_3 \end{aligned} \tag{3}$$

where c_i, s_i correspond to $\cos(\theta_i)$ and $\sin(\theta_i)$ respectively, and x_{offset} is the known horizontal distance from the rotation point of the treadmill to the zero position of the linear track.

These two equations were then solved for the two unknown variables $\|\mathbf{R_3}\|$ and θ_3 in terms of the inputs θ_1 and x_{track}. It must be noted that an inclinometer was used in order to measure the treadmill angular deflection θ_1, while the position of the linear track x_{track} is controlled in real-time in order to achieve the desired stiffness.

The same method was used in order to describe the kinematics of the spring mechanism, as shown in Fig. 4. The final equations that were solved for the two unknowns $\|\mathbf{R_{1a}}\|$ and θ_{1a} are given by:

$$\begin{aligned} \|\mathbf{R_{1a}}\| \cos(\theta_{1a}) + \|\mathbf{R_{2a}}\| \cos(\theta_3) &= \|\mathbf{R_{3a}}\| \\ \|\mathbf{R_{1a}}\| \sin(\theta_{1a}) + \|\mathbf{R_{2a}}\| \sin(\theta_3) &= \|\mathbf{R_{4a}}\| \end{aligned} \tag{4}$$

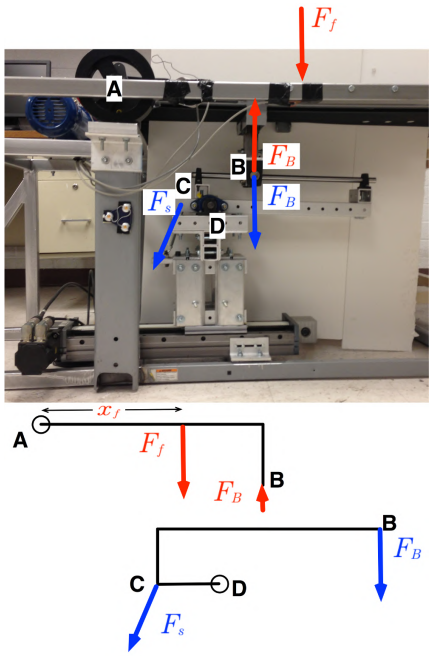

Fig. 5. VST kinetics. F_f is the force exerted by the subject's foot, at a distance x_f from the rotation point of the treadmill. F_s is the spring force and F_B the force at the sliding joint B.

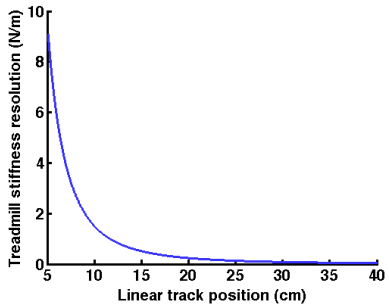

Fig. 6. Treadmill stiffness resolution as a function of the linear track position.

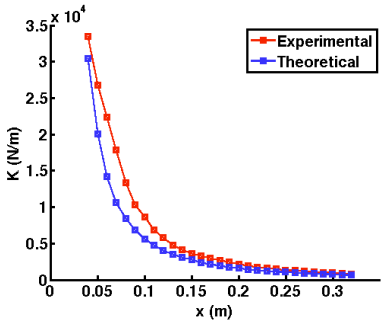

Fig. 7. Experimental vs theoretical values of treadmill effective stiffness.

where all vectors are shown in Fig. 4, along with their correspondence to the real platform features.

2) Kinetics: The final step in the mathematical model of the VST was to use the solutions of unknown variables from the kinematic analysis and apply them to the equilibrium equations for the free body diagrams of the VST, as shown in Fig. 5. F_s is the force exerted by the spring. Since the connection point at B is a sliding joint, the force that it transmits at mechanical equilibrium can only be perpendicular to the sliding axis along $\mathbf{R_3}$. This allowed the calculation of the transmitted force F_B with the following moment equation about location D.

$$\sum \mathrm{M_D}{=}F_s\|\mathbf{R_{2a}}\|sin(\theta_3{-}\theta_{1a}){-}F_B(\|\mathbf{R_3}\|-\|\mathbf{R_5}\|){=}0 \tag{5}$$

where $F_s{=}2k(\|\mathbf{R_{1a}}\|-\mathrm{l_0})$ is the force from the springs and l_0 is the rest length of the two springs we used, each one having a stiffness k. The calculated value for F_B was used to solve for the force of the foot F_f in the equilibrium equation about point A:

$$\begin{aligned}\sum \mathrm{M_A}{=}&F_B\|\mathbf{R_1}\|cos(\theta_3{-}\theta_1)\\ &{-}F_B\|\mathbf{R_2}\|sin(\theta_3{-}\theta_1){-}F_f x_f cos(\theta_1){=}0\end{aligned} \tag{6}$$

Then, the effective stiffness of the treadmill k_t is finally computed by:

$$k_t{=}\frac{F_f}{x_f\tan(\theta_1)} \tag{7}$$

The mathematical derivation above shows that the effective treadmill stiffness at the location of the subject's foot can be calculated by measuring the angle of the treadmill deflection θ_1, the foot position x_f and the track position x_{track}. The latter is something that we control, therefore, given the position of the subject's foot and the angular deflection of the treadmill, the control variable of the system is the position of the track x_{track}.

The range of the control of the track position will define the range of the treadmill effective stiffness that we can achieve. For $x_{track} = 0$, the treadmill stiffness is practically infinite, since the treadmill can not be deflected. For the maximum displacement of the track of $40cm$, the computed treadmill stiffness, assuming that the foot of the subject is approximately in the middle of the treadmill (i.e. during mid-stance), is $585.5N/m$. At the end of the treadmill (i.e. at toe-off phase), the minimum achievable stiffness is $61.7N/m$.

The resolution of achievable displacement of the linear track is $0.01mm$. Since the relationship between the linear track position and the treadmill effective stiffness in non-linear, the resolution of achievable treadmill stiffness is dependent on the linear track position. By solving the aforementioned equations and using the given linear track resolution, we can compute the resolution for stiffness for any given linear track position. This solution curve is depicted in Fig. 6, where it is shown that the resolution of stiffness can range from $9.06N/m$ when the linear track is at $5cm$, to $0.038N/m$ when the linear track is at its maximum displacement of $40cm$. Lower resolution is achieved for position between 0 and $5cm$ of the linear track, as stiffness grows to infinity.

D. Experimental Validation

The results obtained from the mathematical model were compared to experimental data for validation. The apparent

stiffness of the treadmill for $1cm$ interval displacements of the linear track was found by placing a known mass ($4.5kg$) at a known distance ($0.33m$) along the treadmill and measuring the angular displacement of the treadmill. This process resulted in a plot of stiffness vs. the track position. The resulting curve was compared to the theoretical model where the foot position x_f was defined as $0.33m$ to match the experimental setup. The results are shown in Fig. 7. It can be observed that both models achieve the same type of inverse square power profile and converge at low stiffnesses. The slightly higher stiffness values from the experimental data in parts of the domain may reflect the fact that friction is not accounted for in the theoretical model. Friction would cause a decrease in deflection for a given force resulting in higher stiffness values than a frictionless model. However, our theoretical model matched the experimental one very well, proving the validity of our system. This plot also gives an indication of the range of achievable stiffness as a function of the linear track position.

E. Additional Components

1) Force sensor mat: In order to track the location of the subject's foot, an array of eight force sensing resistors was placed beneath the treadmill belt. Whichever sensor is underneath the center of pressure of the foot will give the highest force reading. When two sensors give similar high force measurements, we can assume that the center of pressure is between the two sensors. Given that the sensor mat spans $80cm$, with our eight sensors, we have a spatial resolution of $5cm$. Assuming that the average human foot length is about $23.5cm$ [19], this resolution is sufficient to know the location of the foot. As was shown in the mathematical derivation above, the foot position is used as an input to calculate the corresponding linear track position that will create the proper apparent stiffness beneath the subject. The force sensor mat is shown in Fig. 1, part C.

2) Split-belt treadmill: The VST employs a split-belt treadmill configuration in order to allow each belt to deflect different amounts. This will allow different force perturbations to be applied to each leg. The treadmill belts are supported $70cm$ above the floor on a frame of steel tubing that permits each belt to independently deflect downward to a maximum of $30°$ from the horizontal position. The adjustability of the treadmill stiffness is currently limited to only one belt, but can be applied to both sides by installing another variable stiffness mechanism. The split belt treadmill is shown in Fig. 1, part D.

3) Treadmill motor: A 1-HP variable speed DC motor (Anaheim Automation, Part Number: BDA-56C-100-90V-1800) drives the treadmill belts. We can obtain speeds of up to $1.85m/s$ at a resolution of $7mm/s$. This includes the average preferred walking speed of $1.2-1.4m/s$ [16], [17], but can be slowed for individuals in therapy or rehabilitation applications. The treadmill motor is shown in Fig. 1, part E.

4) Counterweight: One necessary component to ensure accurate control of treadmill stiffness is a counterweight system to eliminate moments from the treadmill's weight. This is achieved by fastening a weighted slider at the precise location along a co-linear beam (attached to the side of the treadmill platform) which will induce an equal and opposite moment to that of the treadmill at any inclination of the treadmill. The counterweight is shown in Fig. 1, part F.

5) Body weight support: Separate from the treadmill structure, there is a custom-built body weight support designed by LiteGait. By adjusting the height of the support system, we can choose to have full or partial body-weight support. This is an important capability to reduce ground reaction forces to allow more accurate control of force perturbations. In addition, the support increases safety and extends the system's capabilities to stroke patients and other individuals with decreased mobility and stability. Two load-cells attached on the body-weight support harness measure the subject's weight supported by the mechanism from each side. The body weight support and the loadcells are shown in Fig. 1, parts G and H respectively.

III. Results

In order to test the device with healthy subjects and to validate its performance, we conducted some experimental studies, as "proof of concept" for the device. For our preliminary experiments, two healthy males walked on the treadmill moving at a comfortably slow speed of $0.45m/s$ with three different treadmill stiffnesses: 100, 60, and 20 kN/m. This range resembles that of other variable stiffness devices [13], [14], [20]–[22]. The stiffness was kept constant throughout the gait cycle. The provided body weight supported was controlled at approx. 40%. The kinematic data was obtained using a motion capture system (3D Investigator, Northern Digital) that was used to track five markers located at the torso, hip, knee, ankle, and toe in order to calculate the joint angles throughout the gait cycle.

The averaged kinematic data across both subjects is shown in Fig. 8. The hip flexion-extension, knee flexion-extension and ankle dorsi/plantar flexion are shown (mean and standard deviation across all gait cycles). The data is plotted as a function of the gait cycle percentage, where 0% corresponds to heel-strike, 60% corresponds to toe-off etc. As can be seen, the joint angle profiles resemble that of normal gait [18], therefore our system did not alter the normal gait kinematics. The knee and hip kinematics appear to be unaffected by the effective treadmill stiffness changes, while the ankle joint appears to have some systematic increased plantar flexion before toe-off, as the effective treadmill stiffness is lowered. This is expected since the loading of the foot between heel-off and toe-off will press the treadmill downwards at lower stiffness, and therefore the ankle will need to plantar-flex more. Additional studies will be conducted in order to further investigate the effects of stiffness on gait kinematics.

IV. Conclusions

This paper presented the VST device that has been developed with several advantages over existing devices for gait research. The VST can alter the walking surface stiffness in real time, offering a wide range of available stiffness,

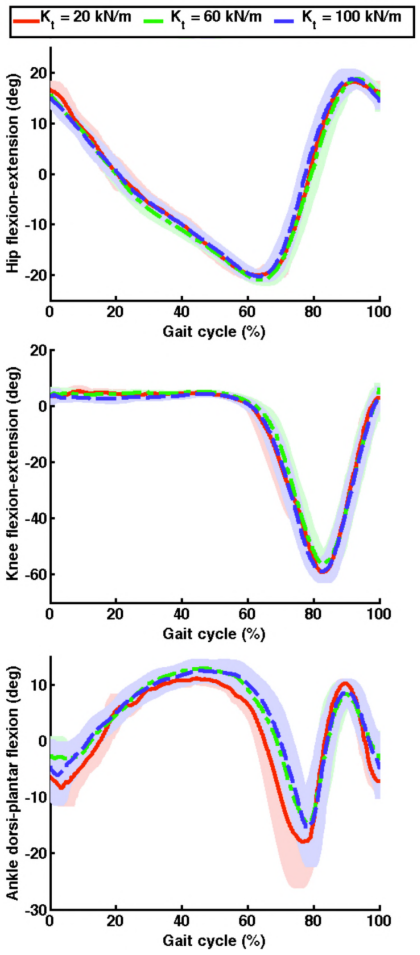

Fig. 8. Averaged kinematic data of hip flexion (+) - extension (-), knee flexion (-) - extension (+) and ankle dorsi (+) - plantar (-) flexion in three cases of treadmill stiffness. Mean (solid lines) and standard deviations (shaded areas) values are shown.

practically from infinite stiffness (non-compliant walking surface) to as low as $61.7N/m$. The resolution of the controlled stiffness can research a maximum of $0.038N/m$, while the effective stiffness can change from maximum to minimum in $0.13s$. All those characteristics make the VST a unique research platform. Unlike previous devices, the VST is capable of creating any profile of stiffness during an experiment and throughout the gait cycle.

Apart from a unique research tool, the VST can be applied for gait rehabilitation. The ability to apply perturbations and regulate force feedback allows for the definition of rehabilitation protocols beyond the state of the art, where the interplay of the leg dynamics with a dynamic environment will play a major role. Moreover, the VST can be used as a simulation-testing device for biological and artificial walkers, when investigating walking patterns and architectures in environments of variable stiffness is required.

REFERENCES

[1] R. af Klint, N. Mazzaro, J. B. Nielsen, T. Sinkjaer, and M. J. Grey, "Load rather than length sensitive feedback contributes to soleus muscle activity during human treadmill walking," *Journal of neurophysiology*, vol. 103, no. 5, pp. 2747–2756, 2010.

[2] M. J. Stephens and J. F. Yang, "Loading during the stance phase of walking in humans increases the extensor emg amplitude but does not change the duration of the step cycle," *Experimental Brain Research*, vol. 124, no. 3, pp. 363–370, 1999.

[3] J. F. Yang, M. J. Stephens, and R. Vishram, "Transient disturbances to one limb produce coordinated, bilateral responses during infant stepping," *Journal of neurophysiology*, vol. 79, no. 5, pp. 2329–2337, 1998.

[4] V. Dietz, A. Gollhofer, M. Kleiber, and M. Trippel, "Regulation of bipedal stance: dependency on "load" receptors," *Experimental brain research*, vol. 89, no. 1, pp. 229–231, 1992.

[5] V. Dietz, R. Müller, and G. Colombo, "Locomotor activity in spinal man: significance of afferent input from joint and load receptors," *Brain*, vol. 125, no. 12, pp. 2626–2634, 2002.

[6] V. Dietz and J. Duysens, "Significance of load receptor input during locomotion: a review," *Gait & posture*, vol. 11, no. 2, pp. 102–110, 2000.

[7] M. Faist, C. Hoefer, M. Hodapp, V. Dietz, W. Berger, and J. Duysens, "In humans ib facilitation depends on locomotion while suppression of ib inhibition requires loading," *Brain research*, vol. 1076, no. 1, pp. 87–92, 2006.

[8] Y. P. Ivanenko, R. Grasso, V. Macellari, and F. Lacquaniti, "Control of foot trajectory in human locomotion: role of ground contact forces in simulated reduced gravity," *J. Neurophysiol.*, vol. 87, pp. 3070–3089, 2002.

[9] M. J. Grey, J. B. Nielsen, N. Mazzaro, and T. Sinkjær, "Positive force feedback in human walking," *The Journal of physiology*, vol. 581, no. 1, pp. 99–105, 2007.

[10] D. S. Marigold and A. E. Patla, "Adapting locomotion to different surface compliances: neuromuscular responses and changes in movement dynamics," *Journal of neurophysiology*, vol. 94, no. 3, pp. 1733–1750, 2005.

[11] M. J. MacLellan and A. E. Patla, "Adaptations of walking pattern on a compliant surface to regulate dynamic stability," *Experimental brain research*, vol. 173, no. 3, pp. 521–530, 2006.

[12] M. D. Chang, E. Sejdić, V. Wright, and T. Chau, "Measures of dynamic stability: detecting differences between walking overground and on a compliant surface," *Human movement science*, vol. 29, no. 6, pp. 977–986, 2010.

[13] T. A. McMahon and P. R. Greene, "The influence of track compliance on running," *Journal of biomechanics*, vol. 12, no. 12, pp. 893–904, 1979.

[14] A. E. Kerdok, A. A. Biewener, T. A. McMahon, P. G. Weyand, and H. M. Herr, "Energetics and mechanics of human running on surfaces of different stiffnesses," *Journal of Applied Physiology*, vol. 92, no. 2, pp. 469–478, 2002.

[15] A. Jafari, N. G. Tsagarakis, and D. G. Caldwell, "AwAS-II: A new Actuator with Adjustable Stiffness based on the novel principle of adaptable pivot point and variable lever ratio," in *Robotics and Automation (ICRA), 2011 IEEE International Conference on*, 2011, pp. 4638–4643.

[16] R. C. Browning, E. A. Baker, J. A. Herron, and R. Kram, "Effects of obesity and sex on the energetic cost and preferred speed of walking," *Journal of Applied Physiology*, vol. 100, no. 2, pp. 390–398, 2006.

[17] R. V. Levine and A. Norenzayan, "The pace of life in 31 countries," *Journal of cross-cultural psychology*, vol. 30, no. 2, pp. 178–205, 1999.

[18] J. Perry, J. R. Davids *et al.*, "Gait analysis: normal and pathological function," *Journal of Pediatric Orthopaedics*, vol. 12, no. 6, p. 815, 1992.

[19] R. M. Pawar and M. N. Pawar, "Foot lengtha functional parameter for assessment of height," *The Foot*, vol. 22, no. 1, pp. 31–34, 2012.

[20] C. T. Farley, H. H. Houdijk, C. Van Strien, and M. Louie, "Mechanism of leg stiffness adjustment for hopping on surfaces of different stiffnesses," *Journal of Applied Physiology*, vol. 85, no. 3, pp. 1044–1055, 1998.

[21] D. P. Ferris and C. T. Farley, "Interaction of leg stiffness and surface stiffness during human hopping," *Journal of applied physiology*, vol. 82, no. 1, pp. 15–22, 1997.

[22] D. P. Ferris, K. Liang, and C. T. Farley, "Runners adjust leg stiffness for their first step on a new running surface," *Journal of biomechanics*, vol. 32, no. 8, pp. 787–794, 1999.